Wireless Networks 9, 165–177, 2003

MR^{2}RP: The Multi-Rate and Multi-Range Routing Protocol for IEEE 802.11 Ad Hoc Wireless Networks

SHIANN-TSONG SHEU *
Department of Electrical Engineering, Tamkang University, Tamsui, Taipei, Taiwan, ROC

YIHJIA TSAI and JENHUI CHEN
Department of Computer Science and Information Engineering, Tamkang University, Tamsui, Taipei, Taiwan, ROC

Abstract. This paper discusses the issue of routing packets over an IEEE 802.11 *ad hoc* wireless network with multiple data rates (1/2/5.5/11 Mb/s). With the characteristics of modulation schemes, the data rate of wireless network is inversely proportional with the transmission distance. The conventional shortest path of minimum-hops approach will be no longer suitable for the contemporary multi-rate/multi-range wireless networks (MR^{2}WN). In this paper, we will propose an efficient delay-oriented multi-rate/multi-range routing protocol (MR^{2}RP) for MR^{2}WN to maximize the channel utilization as well as to minimize the network transfer delay from source to destination. By analyzing the medium access delay of the IEEE 802.11 medium access control (MAC) protocol, the proposed MR^{2}RP is capable of predicting the transfer delay of a routing path and finding the best one, which has the minimum transfer delay from source to destination. The proposed MR^{2}RP may choose a longer path but with less contention competitors and buffer queuing delay. Simulation results show that MR^{2}RP performs the load balancing and fast routing very well, and its call blocking probability is obviously lower than that of conventional minimum-hops approach with fixed transmission rate.

Keywords: ad hoc, local area network (LAN), medium access control (MAC), routing, wireless

1. Introduction

As wireless services become ever more ubiquitous, there is an increasing demand for the provision of the multimedia services over wireless networks. Wireless applications are becoming popular for high-speed communications over small areas, where wiring for conventional networking is difficult or not economic. A wireless *ad hoc* network is a collection of mobile hosts (MHs), which forms a temporary network without the aid of any pre-established infrastructure or centralized administration. The IEEE 802.11 standard provides detailed medium access control (MAC) and physical (PHY) layer specifications for wireless local area networks (WLANs) [14]. This standard includes a basic distributed coordination function (DCF) and an optional point coordination function (PCF). The DCF uses carrier sense multiple access with collision avoidance (CSMA/CA) as the basic channel access protocol to transmit asynchronous data in the contention period. This contention-based MAC protocol cannot guarantee transfer delay for multimedia services. By employing the PCF, the service delay bound can be guaranteed. However, the PCF is a polling-based protocol, which is not designed for the distributed environment. Furthermore, in IEEE 802.11 *ad hoc* WLAN, the diameter of the basic service area (BSA) of an independent basic service set (IBSS) is only considered on the order of 100 feet [6]. This implies that all MHs in the *ad hoc* WLAN are able to communicate with each other directly. In fact, any movable MH may cross the transmission boundary of BSA and the packets from/for them must be relayed via some intermediate MHs [16,23,26,29]. Thus, the critical problem is how to find a reliable route with delay constraint from source to destination. Unfortunately, IEEE 802.11 standard does not provide any solution for this complicated multi-hop routing problem.

Recently, adaptive transmission techniques have been extensively investigated for the improvement of transmission performance in wireless communications. These techniques vary the transmission power [13], transmission packet length [8,21,31] coding rate/scheme [34], and modulation technology [1,15,27,35,37] under the time-varying channel. For instances, papers [1,35] varied the constellation size according to different kinds of channel conditions to get better transmission performance. In [27], authors studied the theoretical performance limitation of adaptive modulation with and without power control. In [15,37] different adaptive modulations were investigated with the dynamic channel allocation (DCA) technology. Besides, the variable-rate quadrature amplitude modulation (QAM) schemes also have been proposed in several third-generation wireless communication systems [7]. All of them are trying to improve the effective data rate under the specified bit error rate (BER).

In [37], authors proposed the concept that throughput could be increased by permitting MH, which nears the central of the cell, to use the high-level modulation scheme. In contract, MH nears the fringes of the cell has to use the low-level (e.g., binary) modulation to cope with the lower signal to noise ratio (SNR). The same concept has also been proposed in [2,3,36]. Similarly, Harris and Lucent companies have proposed high data rate modulation scheme "Com-

* Corresponding author.

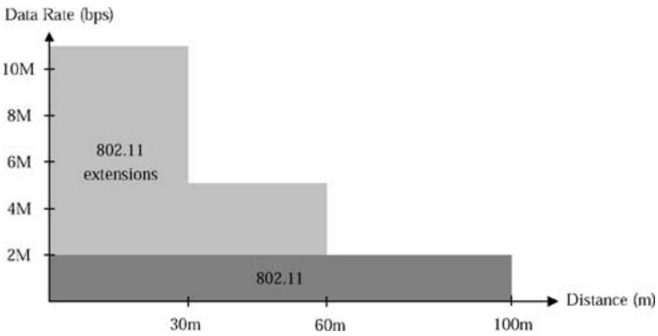

Figure 1. The data rate versus transmission range in IEEE 802.11 standard.

plementary Code Keying" (CCK) [4,9,12], which was referred from the "Complementary Code" [11,32,33]. The IEEE working group (WG) to support data rate up to 11 Mb/s has finally adopted the CCK. To provide the interoperability for existing networks, Harris proposed a baseband processor [9] that has the ability to provide four different modulation schemes: DBPSK, DQPSK, CCK, and MBOK. Based on these schemes, four different data rates (1/2/5.5/11 Mb/s) are supported in WLANs.

In such multi-rate WLAN, the maximal data rate may not always be adopted due to the transmission distance between MHs is contra-proportional with the data rate. The general concept is that a higher-level modulation scheme requires a higher SNR to obtain the same specified BER in respect to a lower level modulation scheme. That is, the maximal data rate of a modulation scheme will be obtained only when the distance between two transceivers is not over its transmission distance boundary. In [3], the longest transmission distances of data rates 11 Mb/s, 5.5 Mb/s, 2/1 Mb/s are identified as 30 m, 60 m and 100 m, respectively. The detail relationships between data rates and the transmission distances are shown in figure 1. For simplicity, such multi-rate/multi-range IEEE 802.11 wireless *ad hoc* network is denoted as MR^{2}WN in this paper.

In MR^{2}WN, two adjacent MHs may deliver packets to each other at several transmission rates. Therefore, the shortest path of minimal hops may not be the fast route from source to destination. The way of finding the reliable route from source to destination with minimal transfer delay in MR^{2}WN becomes more difficult than conventional *ad hoc* WLAN. In this paper, we will propose a multi-rate and multi-range routing protocol (MR^{2}RP) for MR^{2}WN to maximize channel utilization as well as to minimize the transfer delay.

The remainder of this paper is organized as follows. Section 2 briefly describes the operations of the DCF in the IEEE 802.11 standard and the PLCP sublayer also be introduced in this section. In section 3, we discuss the multi-hop routing in MR^{2}WN and the proposed MR^{2}RP is introduced at the same time. The MAC delay in IEEE 802.11 CSMA/CA protocol is also estimated in this section. Simulation models and results are shown in section 4. Finally, we will give some conclusions and remarks in section 5.

2. The IEEE 802.11 MAC protocol

This section will briefly summarize the DCF of the IEEE 802.11 MAC protocol.

2.1. The IEEE 802.11 distributed coordination function

The DCF uses CSMA/CA as the basic channel access protocol to transmit asynchronous data in the contention period. When a MH desiring to transmit frames, it needs monitor the channel activity before its transmission. If the MH perceives that channel is idle for a time period equal to a distributed inter-frame space (DIFS), it will trigger a random backoff delay before transmission (this is the 'collision avoidance' feature of the CSMA/CA protocol). Otherwise, the station persists on monitoring the channel until it detects channel idle for the DIFS duration. (The backoff time is measured in *slot time* (denoted as η in abbreviation), which is defined as the time needed for a node to detect a packet, to accumulate the time needs for the propagation delay, the time needed to switch from the receiving state to the transmitting state, and the time to signal to the MAC layer the state of the channel (busy detect time).) The random backoff procedure can efficiently minimize the collision probability. In addition, to avoid channel capture, a MH must wait a random backoff time between two consecutive frame transmissions even if the medium is sensed idle for the DIFS period after precedent transmission. As an exception to this rule, the protocol provides a fragmentation mechanism, which allows a MH to transmit a number of MAC protocol data units (MPDUs) successively without performing the backoff delay. The only constraint is that these fragmented MPDUs are belonging to a same PDU in the upper protocol layer. These fragments are then transmitted in sequence, with only a short inter-frame space (SIFS) between them, so that only the first fragment must contend for the channel access. Obviously, the SIFS should be shorter than DIFS.

For each frame transmission, the DCF defines an optionally four-way handshaking scheme as shown in figure 2. This scheme uses request to send (RTS) and clear to send (CTS) control frames to overcome the well-known hidden terminal problem [19] and to provide virtual carrier sense for saving battery power [10]. The duration field in the MAC header of a control/data frame is used to carry the information of time period requested for a complete transmission. Any MH receives this information, it will update its network allocation vector (NAV) which contains the information of the interval the channel will remain busy. In this paper, we assume that each data transmission should first issue the RTS frame and CTS frame at the lowest data rate, and follow by an acknowledgment (ACK) frame. To prevent the handshaking process from disturbing by other transmissions, the SIFS is also used to guarantee the control frames to have a higher priority than data frames.

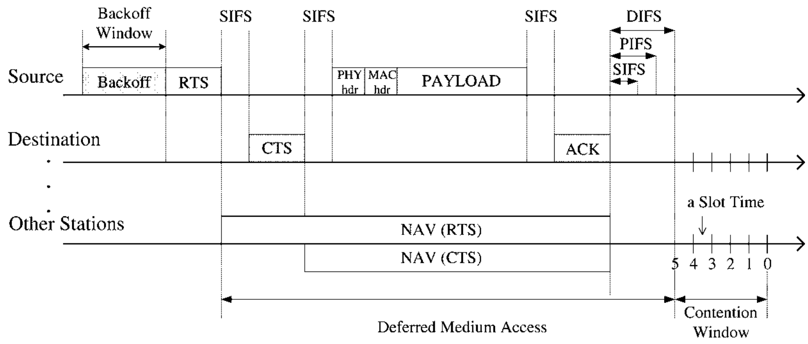

Figure 2. An illustration of RTS/CTS and backoff mechanism of DCF.

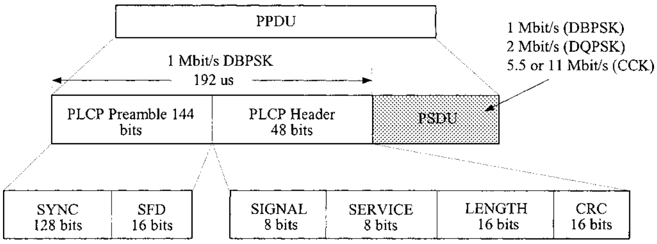

Figure 3. Long PLCP PPDU format.

2.2. The PLCP sublayer

The IEEE Std 802.11/b provides a multi-rate transmission scheme as MAC protocol. To allow the MAC to operate with minimum dependence on the physical medium dependent sublayer, a physical layer convergence procedure (PLCP) sublayer is defined. This function simplifies the PHY service interface to the MAC services. This subclause provides a convergence procedure for the 2, 5.5, and 11 Mb/s specification, in which PLCP service data units (PSDUs) are converted to and from physical protocol data units (PPDUs). Before transmission, the PSDU will be appended with a PLCP preamble and header to create the PPDU. Two different preambles and headers are defined: the mandatory supported long preamble and header, which interoperates with the current 1 Mb/s and 2 Mb/s Direct Sequence Spread Spectrum (DSSS) specification (as described in [14]), and an optional short preamble and header. At the receiver, the PLCP preamble and header are processed to aid in demodulation and delivery of the PSDU. Figure 3 shows the format for the interoperable (long) PPDU, including the PLCP preamble, the PLCP header, and the PSDU. The PLCP preamble contains two information: synchronization (SYNC) and start frame delimiter (SFD). The PLCP header contains the following fields: signaling (SIGNAL), service (SERVICE), length (LENGTH), and CCITT CRC-16. A short PLCP preamble and header (HR/DSSS/short) is defined as optional. Although short preamble and header may be used to minimize overhead and, thus, maximize the network data throughput, but we do not consider in this paper. This is because that a transmitter using the short PLCP will only be interoperable with another receiver that is also capable of receiving this short PLCP. To interoperate with a receiver that is not capable of receiving a short preamble and header, the transmitter shall use the long PLCP preamble and header.

3. The multi-rate and multi-range routing in multi-hop ad hoc WLANs

3.1. Multi-hop ad hoc WLANs

When the network population is large, all MHs are virtually partitioned into clusters so that the bandwidth can be utilized efficiently. Generally, a cluster is defined as a number of MHs, which can directly transmit/receive packet to/from each other and content the bandwidth. A MH is allowed to belong to many clusters at any time. Since all members of a cluster share the channel resource, member in a larger cluster will have a higher probability of suffering a longer MAC delay.

The most important issue in a multi-hop *ad hoc* WLAN is how a MH to communicate with another MH, which is not in its direct transmission range. Intuitively, some intermediate hosts must involve in relaying packets from source to destination. The critical problem is how to find an efficient and reliable route [29] from source to destination. The common approach is the shortest-path routing. The well-known algorithm is the distributed Bellman–Ford (DBF) algorithm [22], In DBF, every host maintains the length (cost) of the shortest path from each of its neighbor hosts to every destination. With this information, a host sends data packets to a neighbor, which leads to a shortest path to the destination. In order to maintain up-to-date distance information in a dynamic environment, every host monitors its outgoing links and periodically broadcasts to neighboring hosts its current estimation of the shortest distance to every network destination.

The most commonly used measurement of distance is the number of hops in the path. Even though this measure is easy to compute, it cannot reflect the influences on realistic access delay. This is because that a routing algorithm, which is based on such a distance measurement, may route packets over a few popular paths in network. This will result in serious congestion in network, especially in the wireless network with limited bandwidth capacity. Taking figure 4, for example, if MH_2 wants to send packets to MH_9, the shortest path of the minimum hops will be the path (MH_2, MH_4, MH_6, MH_9). Along this path, when MH_6 relays packets, it needs to contend the air channel with the other six neighbors (MH_3, MH_4,

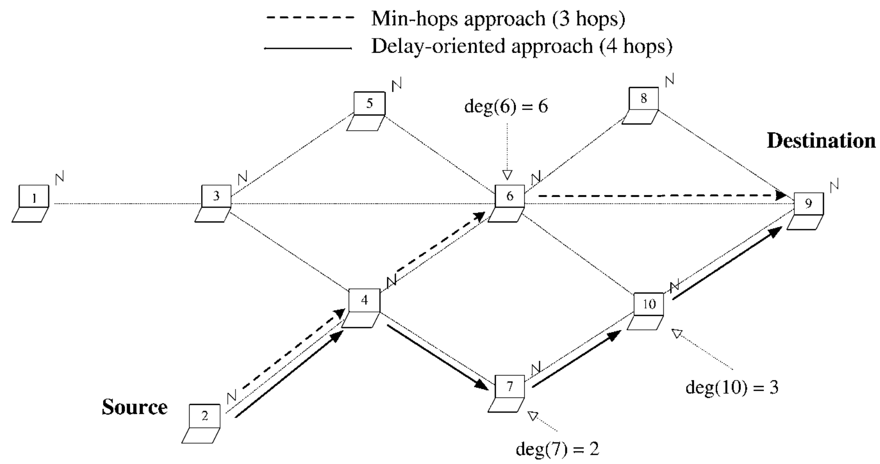

Figure 4. An example of multi-hop routing in wireless *ad hoc* network.

MH_5, MH_8, MH_9, MH_{10}). This will spend a long time to solve the channel contention by any contention-based protocol. On the contrary, if we select the path (MH_2, MH_4, MH_7, MH_{10}, MH_9) with 4 hops, the relayed packets have a better chance to quickly reach destination. Therefore, it is desired to design a delay-oriented shortest path routing protocol for IEEE 802.11 wireless *ad hoc* networks to perform load balancing to maximize channel utilization as well as to minimize transfer delay.

3.2. The multi-rate and multi-range transmission model

For simplicity, we assume the PHY in MR^2WN be able to support three transmission rates TR_h, TR_m and TR_l ($TR_h > TR_m > TR_l$), and the maximal transmission distances of them are denoted as TD_h, TD_m and TD_l ($TD_h < TD_m < TD_l$), respectively. Figure 5 shows three possible transmissions from MH_0 in a MR^2WN. We note that MH_0 can transmit packets to MH_1 by any one of data rates since the transmission distance is less than TD_h. However, in the case of transmitting packets from MH_0 to MH_n, it can only use the lowest data rate TR_l. Therefore, in MR^2WN, a longer hopping will shorten the transmission distance of a path but sacrificing the transmission speed. Instructively, one may choose the path of the maximal transmission rate to minimize the transfer delay. Nevertheless, too many times of relaying a packet in MR^2WN is not a smart solution because of the increasing of contention delay and buffer delay. Besides, transmitting a packet several times in the network will degrade the network throughput significantly. As a result, it is a tradeoff between the channel utilization and transmission speed in MR^2WN.

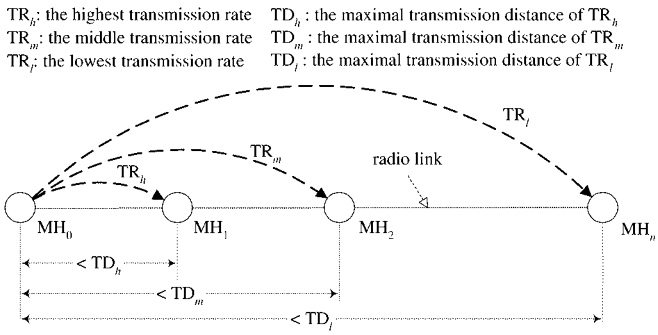

Figure 5. Multi-rate transmissions in MR^2WN.

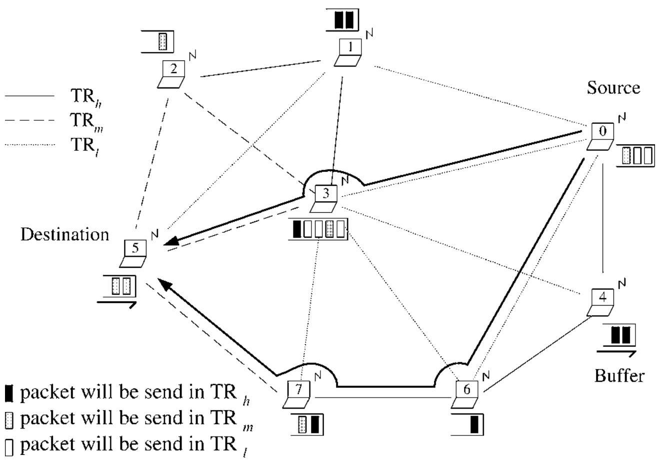

Figure 6. An example of multi-rate transmission approach versus minimum hop approach.

Figure 6 shows an example of routing packets from MH_0 to MH_5. By minimal-hops (Min-hops, for short) approach, path (MH_0, MH_3, MH_5) of two hops will be chosen. However, path (MH_0, MH_6, MH_7, MH_5) of three hops will provide a faster route than the previous one (we will prove this later). That is, even though the former path is one hop shorter than the latter path and the transmission rates of the first and the last link in two paths are the same, the total transfer delay of the latter path is still smaller than that of the former path. The reason is that not only the MAC delay but also the buffer queueing delay incurred in every relaying host will affect the total transfer delay. The MAC delay of a contending MH is strongly depending on the number of competitors in cluster. The buffer queueing delay of a host is depending on the amount of buffered packets in it and the transmission rate assigned for each of them. This implies that a buffer with a shorter queue length does not mean it will provide less queueing delay in MR^{2}WN. In this following subsection, we will present how the proposed multi-rate and multi-range routing protocol (MR^{2}RP) to precisely estimate delays and find the optimal route for each transmission request.

3.3. The multi-rate and multi-range routing protocol (MR^{2}RP)

Before describing the MR^{2}RP protocol, three critical problems must be solved: (1) In order to find the best route with minimal transfer delay, the MR^{2}RP needs collect all network information on time. (2) The MR^{2}RP needs to predict the precise MAC delay of a MH in WLANs. (3) According to the estimated MAC delay and the information of how many packets queued in buffer of a node, the MR^{2}RP estimates the precise transmission cost for making the routing decision.

Employing some well-known on-demand routing protocols (for instances, the dynamic source routing (DSR) [16] or the *ad hoc* on-demand distance vector (AODV) [26] routing protocols) can solve the first problem. In these protocols, the routes are established on data transmission demand by a source MH. In the DSR algorithm, the source MH determines the complete sequence of MHs in the routing path. In wireless network, since the network connectivity is changing from time to time, one may use a route-discovery protocol to dynamically construct the source routes. That is, whenever a MH needs a route to another MH and it does not have one in its cache, it dynamically determines one by flooding the network with route-discovery packets. Another approach is by using table-driven algorithm; each MH maintains information for each known destination in the network and updates its routing-table entries as needed. The destination-sequenced distance-vector routing (DSDV) protocol described in [25] is a table-driven algorithm based on the classical Bellman–Ford routing mechanism. The wireless routing protocol (WRP) described in [23] is a table-based protocol with the goal of maintaining routing information among all MHs in the network.

A variant approach of on-demand routing is the hybrid on-demand and table-driven routing. This type of routing also creates routes only when the source MH desires to transmit packet. For example, the AODV routing protocol builds on the described DSDV algorithm is an improvement on DSDV because it typically minimizes the number of required broadcasts by creating routes on a demand basis, as opposed to maintaining a complete list of routes as in the DSDV algorithm. When a source MH desires to send a message to some destination MH and does not already have a valid route to that destination, it initiates a path discovery process to locate the other MHs. To do this, it broadcasts a route request (RREQ) packet to its neighbors, which then forward the request to their neighbors with a fresh route to the destination. During the routing process, intermediate MHs piggyback their load information on RREQ packet and then rebroadcast it. The approach utilizes sequence numbers to ensure all reachable routes are loop-free. Each MH maintains its own sequence number as well as a broadcast ID. The broadcast ID is incremented for every RREQ the MH initiates. Combining the broadcast ID with the MH's address, one can uniquely identify an RREQ. Note that all RREQ packets are sent in 2 Mb/s data rate since the lowest data rate will make a more number of neighbors receive RREQ requests.

During the process of forwarding the RREQ, intermediate MHs will update their route tables the address of the neighbor from which the first copy of the broadcast packet is received. If additional copies of the same RREQ are later received, those load information in these packets are compared and updated in the routing table. Once the RREQ reaches the destination or an intermediate MH with a fresh enough route, the destination/intermediate MH responds by unicasting a route reply (RREP) packet back to the neighbor from which it first received the RREQ. The RREP packet will be sent at the maximum transmission rate between this MH and previous MH. As the RREP is routed back along the reverse path, MHs along this path set up forward route entries in their route tables that point to the MH from which the RREP came. These forward route entries indicate the active forward routes. Each route entry is associated a route timer, which will cause the deletion of the entry if it is not referred within the specified lifetime. This is the way employed in the proposed MR^{2}RP to maintain the routing table. Because the RREP is forwarded along the path established by the RREQ, MR^{2}RP only supports the use of symmetric links. Since the on demanding approach needs take a considerable time to find the path, an additional aspect of our MR^{2}RP protocol is the use of hello messages. MR^{2}RP protocol needs periodically broadcast hello messages in lowest transmission rate to inform every neighboring MH. By the RREQ and hello messages, every MH can collect whole network information by wasting some bandwidth.

The second problem can be solved by analyzing the access delay in the CSMA/CA protocol. In order to calculate the access delay and find the available path, each station needs the connectivity information of the network. This *connectivity matrix* (*CM*), which can be derived from the routing table as mentioned above, is defined as follows.

Connectivity matrix: $CM_{ij} = \{cm(i, j)_{N\times N} \mid 1 \leqslant i, j \leqslant N\}$, where $cm(i, j) = k$, $k \in \{0, 1, 2, 3\}$. Element $cm(i, j) = k$ $(k > 0)$ indicates that MH_i can transmit packets to MH_j at transmission rate TR_x $(\forall TR_x \leqslant TR_k)$ directly. Otherwise, MH_i and MH_j cannot hear each other. Thus, we have

$$cm(i, j) = \begin{cases} 1, & \text{the lowest transmission rate } TR_l, \\ 2, & \text{the medium transmission rate } TR_m, \\ 3, & \text{the highest transmission rate } TR_h, \\ 0, & \text{no connectivity.} \end{cases} \tag{3.0}$$

For illustration, we denote TR_h, TR_m and TR_l as TR_3, TR_2 and TR_1, respectively (where $TR_3 > TR_2 > TR_1$). Considering the example shown in figure 4 again, the corresponding

CM matrix is shown as follows.

$$CM = \begin{pmatrix} 0 & 1 & 0 & 1 & 3 & 0 & 1 & 0 \\ 1 & 0 & 3 & 3 & 0 & 1 & 0 & 0 \\ 0 & 3 & 0 & 2 & 0 & 2 & 0 & 0 \\ 1 & 3 & 2 & 0 & 1 & 2 & 1 & 1 \\ 3 & 0 & 0 & 1 & 0 & 0 & 3 & 0 \\ 0 & 1 & 2 & 2 & 0 & 0 & 0 & 2 \\ 1 & 0 & 0 & 1 & 3 & 0 & 0 & 1 \\ 0 & 0 & 0 & 1 & 0 & 2 & 1 & 0 \end{pmatrix}_{N\times N}.$$

The matrix in this example is symmetric. We notice that, in real case, the transmission condition between two MHs may not be the same in both directions. According to the *CM*, every source can apply the Dijkstra algorithm to find the path of minimal hops and the path with the minimal transmission delay (excluding the MAC delay and buffer delay) [5]. To derive the path of minimal hops, when applying the Dijkstra algorithm, every non-zero value and value 0 in *CM* matrix should be treated as value 1 and infinite positive value respectively. The routing algorithm adopted by MR^{2}RP protocol is similar to the Dijkstra algorithm except the cost function on edges. To obtain the path of the minimal total transfer delay from source to destination, we need modify the value of each element in the *CM* matrix as the desired cost value, which is the predicted access delay. Recall the estimated access delay should include the MAC delay, the buffer queueing delay and transmission delay.

3.4. The MAC delay estimation

In estimating delay effect in wireless scenario [30], we need to consider the randomness of both the packet arrival rate and the service time. Since these two parameters are random variables, they are described in statistical terms and thus have a probability distribution associated with each of them.

For the message arrival process, the most common description is given in terms of Poisson statistics [17,24,28]. Poisson statistics are based on a discrete distribution of events. Under the assumption that a system has a large number of independent arrival packets, Poisson statistics state that the probability $P_n(t)$ of exactly n packets arriving a MH during a time interval of length t is given by

$$P_n(t) = \frac{(\lambda t)^n}{n!} \mathrm{e}^{-\lambda t}, \tag{3.1}$$

where λ is the mean arrival rate and $n = 0, 1, 2, \ldots, \infty$.

Hence, the probability of no packet arrives at a MH during the interval time t is

$$P_0(t) = \mathrm{e}^{-\lambda t}. \tag{3.2}$$

In the IEEE 802.11 wireless *ad hoc* networks, stations in a cluster will contend and share the channel bandwidth. Assume there are N MHs (which are indexed from 0 to $N-1$) in MR^{2}WN. Let $|Adj(i)|$ be the number of neighbors of MH_i with maximum transmission distance (TD_l). According to *CM*, the $|Adj(i)|$ can be easily derived by the following equation:

$$\left|Adj(i)\right| = \sum_{j=0}^{N-1} d\bigl(cm(i, j)\bigr), \tag{3.3}$$

$$d(x) = \begin{cases} 1, & \text{if } x \geqslant \mathrm{TD}_l, \\ 0, & \text{otherwise.} \end{cases} \tag{3.4}$$

For simplicity, we let $P_{\mathrm{idle}}^{(i)}(t)$ denote the probability of MH_i successes in sensing channel *idle* in the maximum transmission range with radius TD_l for time interval t. (The $P_{\mathrm{idle}}^{(i)}(t)$ can be treated as the probability that MH_i detects no other MH transmitting data in the cluster during observing time interval t.) Thus, the probability can be derived by

$$P_{\mathrm{idle}}^{(i)}(t) = \mathrm{e}^{-\lambda(i)t}, \tag{3.5}$$

where $\lambda(i)$ is the total packet arrival rate in the cluster of maximum transmission distance respecting to MH_i. The value of $\lambda(i)$ can be derived by the following equation:

$$\lambda(i) = \left|Adj(i)\right| \cdot \lambda. \tag{3.6}$$

Figure 7 illustrates the simplified transition state diagram of mobile host, say MH_i, attempts to transmit packets in the IEEE 802.11 CSMA/CA protocol. The state transition diagram consists of the probability notations as shown in table 1. Initially, MH_i stays in the **IDLE** state. When a packet arrives MH_i (either generates by itself or receives from neighbor for relaying), MH_i will enter into **Arrival** state. In **Arrival** state, if MH_i senses medium busy for SIFS period, it will continuously listen the radio medium until the medium becomes free for a DIFS interval time. If the channel sustains idle for DIFS period, MH_i will enter the **Backoff** state and defer a random backoff time (denoted as $\overline{\mathcal{B}}$) before transmitting. Thus, the mean random backoff time $\overline{\mathcal{B}}$ of a transmission can be evaluated based on IEEE 802.11 MAC protocol. In this paper, we assume the minimum backoff window size $W = 32\eta$ and the maximum window size is 1024η as standard definitions. According to the binary exponential backoff algorithm in CSMA/CA protocol, the backoff delay $b(n)$ of the nth retransmission ($0 \leqslant n \leqslant 5$) can be calculated by the following recursive functions:

$$\begin{aligned} b(0) &= P_{\mathrm{idle}}^{(i)}(\eta)\frac{2^0 \cdot W}{2} + \bigl(1 - P_{\mathrm{idle}}^{(i)}(\eta)\bigr)b(1), \\ b(1) &= P_{\mathrm{idle}}^{(i)}(\eta)\frac{2^1 \cdot W}{2} + \bigl(1 - P_{\mathrm{idle}}^{(i)}(\eta)\bigr)b(2), \\ b(2) &= P_{\mathrm{idle}}^{(i)}(\eta)\frac{2^2 \cdot W}{2} + \bigl(1 - P_{\mathrm{idle}}^{(i)}(\eta)\bigr)b(3), \\ b(3) &= P_{\mathrm{idle}}^{(i)}(\eta)\frac{2^3 \cdot W}{2} + \bigl(1 - P_{\mathrm{idle}}^{(i)}(\eta)\bigr)b(4), \\ b(4) &= P_{\mathrm{idle}}^{(i)}(\eta)\frac{2^4 \cdot W}{2} + \bigl(1 - P_{\mathrm{idle}}^{(i)}(\eta)\bigr)b(5), \\ b(5) &= \frac{2^5 \cdot W}{2} = 2^4 \cdot W. \end{aligned} \tag{3.7}$$

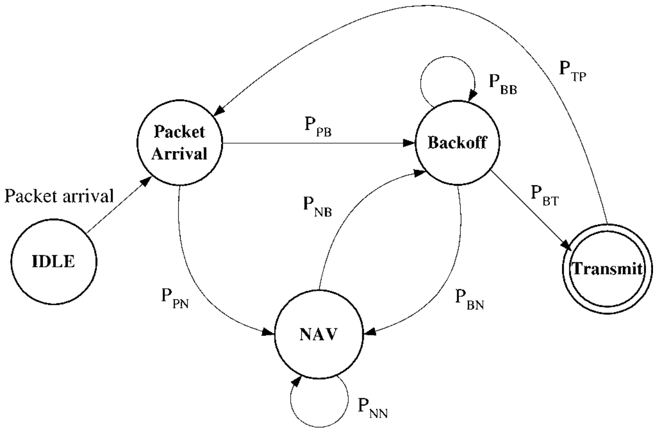

Figure 7. The state transition diagram of IEEE 802.11 CSMA/CA protocol.

Table 1
The description of probability variables in the transition state diagram.

Variable	Description
$P_{AB}^{(i)}$	a station successfully perceives the medium is free within a DIFS time
$P_{AN}^{(i)}$	a station senses the medium is busy within a SIFS time
$P_{NB}^{(i)}$	a station finishes NAV countdown and senses the medium is free for DIFS period
$P_{BN}^{(i,j)}$	a station receives the NAV information from another station when performing back-off countdown
$P_{NN}^{(i)}$	a station receives the NAV information from another stations
$P_{BT}^{(i,j)}$	a station sends RTS packet after finishing its backoff countdown and receives CTS packet from destination station successfully
P_{TA}	a station finishes transmission and returns the initial state

Then, solving equation (3.7) for $\overline{\mathcal{B}}$ leads to

$$\overline{\mathcal{B}} = \sum_{n=0}^{4} \left(P_{\text{idle}}^{(i)}(\eta)\left(1 - P_{\text{idle}}^{(i)}(\eta)\right)^n \cdot 2^{n-1} W\right) + \left(1 - P_{\text{idle}}^{(i)}(\eta)\right)^5 \cdot 2^4 W. \tag{3.8}$$

Therefore, the probability $P_{AB}^{(i)}$ of the state transition from **Arrival** state to **Backoff** state of MH_i with transmission distance TD_l in a DIFS interval can be expressed as

$$\begin{aligned} P_{AB}^{(i)} &\equiv P\{\text{no MHs in cluster transmitting packets during } [t, t + DIFS]\} \\ &= P_{\text{idle}}^{(i)}(DIFS) \\ &= e^{-\lambda(i) DIFS}, \end{aligned} \tag{3.9}$$

where $\lambda(i)$ is the total packet arrival rate in the cluster of maximum transmission radius TD_l respecting to MH_i. The value of $\lambda(i)$ can be derived by the following equation:

$$\lambda(i) = |Adj(i)| \cdot \lambda. \tag{3.10}$$

Otherwise, it will detect the RTS/CTS frame from neighbor MHs and enter the **NAV** state. We note that an idle MH_i will also enter into the **NAV** state after by receiving a RTS/CTS frame. Thus the transition probability $P_{AN}^{(i)}$ from the **Arrival** state to the **NAV** state is equal to the probability of transferring from the **Arrival** state to the **Backoff** state in a DIFS period and can be derived as

$$\begin{aligned} P_{AN}^{(i)} &\equiv P\{\text{MH}_i \text{ senses medium is busy during } [t, t + DIFS]\} \\ &= 1 - P_{AB}^{(i)}(r) = 1 - P_{\text{idle}}^{(i)}(DIFS) \\ &= 1 - e^{-\lambda(i) DIFS}. \end{aligned} \tag{3.11}$$

In the **Backoff** state, MH_i will enter the **Transmit** state as soon as when it finishes the backoff interval countdown and the RTS/CTS frames are transmitted/received successfully. The timing sequence is that, when MH_i finishes the backoff countdown, it will first issue the RTS control frame and then waits for the CTS frame from MH_j to make sure the contention is success or not. Let $P_{BT}^{(i,j)}$ denote the probability that MH_i successes in RTS/CTS handshake with its neighbor MH_j. We have

$$\begin{aligned} P_{BT}^{(i,j)} &\equiv P\{\text{MH}_i \text{ successes in RTS/CTS handshake with receiver } \text{MH}_j\} \\ &= P_{\text{idle}}^{(i)}(2\delta) \cdot P_{\text{idle}}^{(j-(i\cap j))}(RTS + SIFS + 2\delta) \\ &= e^{-\lambda(i)2\delta} \cdot e^{-\Lambda(j)(RTS+SIFS+2\delta)} \\ &= e^{-\lambda(i)2\delta - \Lambda(j)(RTS+SIFS+2\delta)}, \end{aligned} \tag{3.12}$$

where

$$\Lambda(j) = \left(|Adj(j)| - |Adj(i \cap j)|\right) \cdot \lambda \tag{3.13}$$

is the total packet arrival rate in the *shadow* area of cluster, which is the MH_j's transmission area minuses the *intersection* of MH_i and MH_j, denoted as $i \cap j$, during $RTS + SIFS + 2\delta$ interval and δ is the maximum propagation delay from transmitting MH_i to receiving MH_j. Thus, the turnaround time between transmitting MH_i and receiving MH_j is 2δ. We note that the handshaking between MH_i and its neighbor MHs will fail by either collisions occurring when MH_i transmits RTS or when its neighbor MH replies CTS (i.e., the hidden node problem in WLAN is considered in this paper).

During the period of executing backoff countdown, a MH may receive the NAV request from neighbor MHs. In detail, this situation will happen when a neighbor node successfully sends the RTS or the corresponding receiver replies the CTS frame to clear the channel for receiving packet. In this case, MH_i will transit from the **Backoff** state to the **NAV** state. The probability $P_{BN}^{(i,j)}$ can be calculated as

$$\begin{aligned} P_{BN}^{(i,j)} &= 1 - P_{BN}^{(i,j)} \\ &= 1 - e^{-\lambda(i)2\delta - \Lambda(j)(RTS+SIFS+2\delta)}. \end{aligned} \tag{3.14}$$

In this case, MH_i will delay $\overline{\mathcal{N}} = RTS + \delta + SIFS + CTS + \delta + SIFS + T_{\text{data}}^{(r)} + \delta + SIFS + ACK + \delta$ $(= RTS + CTS + ACK + 3SIFS + T_{\text{data}}^{(r)} + 4\delta)$ before its next attempt. Here, notation $T_{\text{data}}^{(r)}$ denotes the required transmission time of transmitting a data packet with mean length L via transmission rate r. We note that the expected NAV defer (denoted as $\overline{\mathcal{N}}$) will also occur on the transition from the **Arrival** state to the **NAV** state and the transition loops in the **NAV** state.

When MH_i finishes counting NAV, it will enter the **Backoff** state after waiting a DIFS interval time. The probabilities $P_{NB}^{(i)}$ can be derived by

$$P_{NB}^{(i)} \equiv P\{\text{MH}_i \text{ finishes NAV countdown and perceives channel idle for DIPS}\} = e^{-\lambda(i)DIFS}. \tag{3.15}$$

Otherwise, MH_i fails in DIFS interval and the probability $P_{NN}^{(i)}$ can be given as

$$P_{NN}^{(i)} = 1 - P_{NB}^{(i)} = -e^{-\lambda(i)DIFS}. \tag{3.16}$$

Now we can solve the expected average MAC delay of a transmission from MH_i to MH_j by transmission rate TR_r in the system (denoted as $E_r^{(i,j)}(M)$). Therefore, from figure 7 we can obtain an expression for the average MAC delay $E_r^{(i,j)}(M)$:

$$E_r^{(i,j)}(M) = P_{AB}^{(i)}\big(DIFS + E_r^{(i)}(B)\big) + P_{AN}^{(i)}\big(DIFS + E_r^{(i)}(N)\big), \tag{3.17}$$

where $E_r^{(i,j)}(B)$ is the additional delay accumulated each time of a transmission from MH_i spending in **Backoff** state, and $E_r^{(i,j)}(N)$ is the delay caused by stay in the **NAV** state. The value for $E_r^{(i,j)}(B)$ can be expressed as follows:

$$E_r^{(i,j)}(B) = P_{BN}^{(i,j)}\big(RTS + SIFS + CTS + \overline{\mathcal{B}} + E_r^{(i,j)}(N)\big) + P_{BT}^{(i,j)}\big(RTS + SIFS + CTS + \overline{\mathcal{B}}\big). \tag{3.18}$$

According to equation (3.14), we have

$$E_r^{(i,j)}(B) = P_{BN}^{(i,j)} E_r^{(i,j)}(N) + RTS + SIFS + CTS + \overline{\mathcal{B}}. \tag{3.19}$$

And the expression for $E_r^{(i)}(N)$ is given by

$$E_r^{(i,j)}(N) = P_{NN}^{(i)}\big(DIFS + \overline{\mathcal{N}} + E_r^{(i,j)}(N)\big) + P_{NB}^{(i)}\big(DIFS + \overline{\mathcal{N}} + E_r^{(i,j)}(B)\big). \tag{3.20}$$

Similarly, according to equation (3.16), we have

$$E_r^{(i,j)}(N) = P_{NN}^{(i)} E_r^{(i)}(N) + P_{NB}^{(i)} E_r^{(i,j)}(B) + DIFS + \overline{\mathcal{N}} \tag{3.21}$$

solving for $E_r^{(i,j)}(N)$ leads to:

$$E_r^{(i,j)}(N) = \frac{DIFS + \overline{\mathcal{N}}}{P_{NB}^{(i)}} + E_r^{(i,j)}(B). \tag{3.22}$$

Substituting equation (3.22) into equation (3.18) leads to:

$$E_r^{(i,j)}(B) = P_{BN}^{(i,j)}\left(\frac{DIFS + \overline{\mathcal{N}}}{P_{NB}^{(i)}} + E_r^{(i,j)}(B)\right) + RTS + SIFS + CTS + \overline{\mathcal{B}}. \tag{3.23}$$

Then solving equation (3.23) gets the following expression:

$$E_r^{(i,j)}(B) = \frac{P_{BN}^{(i,j)}(DIFS + \overline{\mathcal{N}})}{P_{NB}^{(i)} P_{BT}^{(i,j)}} + \frac{RTS + SIFS + CTS + \overline{\mathcal{B}}}{P_{BT}^{(i,j)}}. \tag{3.24}$$

Using equation (3.22) leads to the following expression for $E_r^{(i,j)}(N)$:

$$E_r^{(i,j)}(N) = \frac{DIFS + \overline{\mathcal{N}}}{P_{NB}^{(i)}} + \frac{P_{BN}^{(i,j)}(DIFS + \overline{\mathcal{N}})}{P_{NB}^{(i)} P_{BT}^{(i,j)}} + \frac{RTS + SIFS + CTS + \overline{\mathcal{B}}}{P_{BT}^{(i,j)}} \tag{3.25}$$

and its simplified expression is

$$E_r^{(i,j)}(N) = \frac{P_{NB}^{(i)}(RTS + SIFS + CTS + \overline{\mathcal{B}}) + DIFS + \overline{\mathcal{N}}}{P_{NB}^{(i)} P_{BT}^{(i,j)}}. \tag{3.26}$$

Now substituting the previous two equations (3.24) and (3.26) into equation (3.17) leads to

$$E_r^{(i,j)}(M) = P_{AB}^{(i)}\left(DIFS + \frac{P_{BN}^{(i,j)}(DIFS + \overline{\mathcal{N}})}{P_{NB}^{(i)} P_{BT}^{(i,j)}} + \frac{RTS + SIFS + CTS + \overline{\mathcal{B}}}{P_{BT}^{(i,j)}}\right) + P_{AN}^{(i)}\left(DIFS + \frac{P_{NB}^{(i)}(RTS + SIFS + CTS + \overline{\mathcal{B}}) + DIFS + \overline{\mathcal{N}}}{P_{NB}^{(i)} P_{BT}^{(i,j)}}\right). \tag{3.27}$$

Since, $P_{AB}^{(i)} = P_{NB}^{(i)}$, $P_{AN}^{(i)} = P_{NN}^{(i)}$, and $P_{BN}^{(i,j)} = 1 - P_{BT}^{(i,j)}$. Therefore, we can further simplify the equation (3.27) and get the expected average MAC delay $E_r^{(i,j)}(M)$ as follows:

$$E_r^{(i,j)}(M) = \frac{P_{NB}^{(i)}(RTS + SIFS + CTS + \overline{\mathcal{B}}) + DIFS + \overline{\mathcal{N}})}{P_{NB}^{(i)} P_{BT}^{(i,j)}} - \overline{\mathcal{N}}. \tag{3.28}$$

Figure 8 shows the simulated and analyzed MAC delays of a mobile host under different numbers of neighbor mobile hosts in a cluster. The corresponding system parameters are listed in table 2. Here, we assume that the packet arrival rate per each node λ is 0.001 and the packet mean length is 40 slots (= 200 octets per packet). The DIFS and SIFS interval follow the Direct Sequence Spread Spectrum (DSSS) physical specification in IEEE 802.11 standard and are set to be 2.5 slots (50 μs) and 0.5 slot (10 μs), respectively.

From figure 8, it is clear that the MAC delay is proportional with the number of competitors. The simulation results show that the MAC delays estimated by equation (3.28) are very closed to the simulation results. This implies that the proposed MR^2RP has a good measurement on the MAC delay. Figure 9 shows that how the MAC delays of a mobile host is affected by the number of neighbors, the arrival rates and data rates. We can see that the MAC delay is significantly affected by packet arrival rate. Moreover, the improvement on MAC

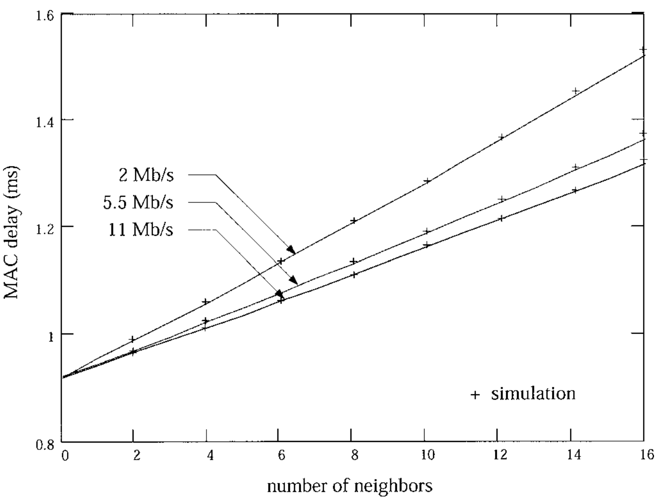

Figure 8. Comparisons of simulated and analyzed average MAC delays of a mobile host under different numbers of neighbor mobile hosts.

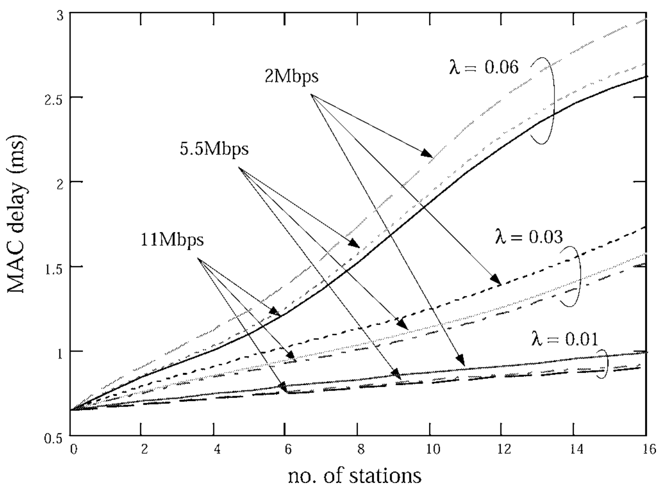

Figure 9. The estimated average MAC delay of a mobile host under different number of neighbor mobile hosts, different arrival rates and different data rates.

Table 2
System parameters in simulations.

Parameter	Normal value
Channel bit rate	2,5.5,11 Mb/s
Transmission range (2 Mb/s)	100 m
Transmission range (5.5 Mb/s)	60 m
Transmission range (11 Mb/s)	30 m
RTS frame length	160 bits
CTS frame length	112 bits
ACK frame length	112 bits
Slot time (η)	20 μs
Air propagation delay (δ)	1 μs
SIFS	10 μs
DIFS	50 μs
PLCP preamble + PLCP header	192 μs
MAC header	34 octets
CWmin	31 slots
CWmax	1023 slots

delay by employing a higher transmission rate will becomes more obvious in a heavy network loaded environment.

3.5. The buffer queuing delay estimation

Even though estimating the MAC delay of relaying host can derive the path of minimal MAC access delay, this path may not be the best path of the minimal end-to-end transfer delay. In [20], they present a so called dynamic load-aware routing (DLAR) protocol that considers intermediate node routing loads as the primary route selection metric. This is mainly resulted from the buffer queuing delay occurring in intermediate host. In multi-hop routing, the buffer delay may dominate the transfer delay of a transmission. To solve this problem, every host needs have the buffer information of each mobile host. This can be collected by exchanging routing information. The buffer information should include the individual queue length of each transmission rate. Let $QB_r(i)$ denote the number of packets which are queuing in buffer with transmission rates TR_r in MH_i ($1 \leqslant r \leqslant 3$). Thus we can get the estimated *transfer delay* (denoted as $D_r(i, j)$) on this link, which route a packet from MH_i to MH_j by transmission rate TR_r, will be

$$D_r(i, j) = \sum_{k=1}^{3}\big(QB_k(i) \cdot E_k^{(i,j)}(M)\big) + E_r^{(i,j)}(M). \quad (3.29)$$

3.6. The routing protocol

Based on the end-to-end transfer delay, we replace every nonzero element in CM by the estimated minimal delay $D_r(i, j)$. (That is, $CM_{ij} = D_{cm(i,j)}(i, j), \forall 1 \leqslant i, j \leqslant N$ and $\lambda = 0.001$.) Now, the shortest path with the minimal delay can be found by also employing the Dijkstra algorithm. (We also note that each element of zero indicates infinite delay cost in Dijkstra algorithm). Take the example shown in figure 6 again. With the system parameters shown in table 2 and queue lengths shown in figure 6, the final CM (measured in ms) for our MR²RP will become

$$CM = \begin{pmatrix} 0 & 4.10 & 0 & 4.27 & 3.76 & 0 & 3.93 & 0 \\ 3.03 & 0 & 2.81 & 3.10 & 0 & 2.92 & 0 & 0 \\ 0 & 1.93 & 0 & 2.07 & 0 & 1.93 & 0 & 0 \\ 5.75 & 5.73 & 5.74 & 0 & 5.75 & 5.74 & 5.75 & 5.75 \\ 2.89 & 0 & 0 & 3.04 & 0 & 0 & 2.89 & 0 \\ 0 & 2.93 & 2.81 & 3.12 & 0 & 0 & 0 & 2.92 \\ 1.92 & 0 & 0 & 2.01 & 1.87 & 0 & 0 & 1.90 \\ 0 & 0 & 0 & 3.11 & 0 & 2.99 & 2.99 & 0 \end{pmatrix}_{8\times 8}.$$

The final CM may not be symmetric since the incurred buffer delay from MH_i to MH_j may different from MH_j to MH_i. According to the conventional shortest path of minimal hop counts, the path (MH_0, MH_3, MH_5) will take $4.27 + 5.74 = 10.01$ ms for every packet to reach destination. On the contrary, using the path (MH_0, MH_6, MH_7, MH_5) for route will lead a lower delay $3.93 + 1.9 + 2.99 = 8.82$ ms. It is apparent that the second path with more hops will gain 1.19 ms for every packet. Let's consider another case in this example where source is MH_0 and the destination is MH_7. The shortest path of Min-hops approach can be either the path (MH_0, MH_3, MH_7) or path (MH_0, MH_6, MH_7). We can see that these two paths have the same hop counts but they will lead to quite different delays. The path (MH_0, MH_6, MH_7) with end-to-end transfer delay 5.83 ms is much better than the path (MH_0, MH_3, MH_7) with total delay 10.02 ms by 4.19 ms. This is because MH_3 is the bottleneck for relaying packets and is often chose as the intermediate host by traditional Min-hops approach.

4. Simulation model and results

To evaluate the effectiveness of the proposed MR^2RP protocol, some simulations were done. In simulations, we considered the realistic system parameters in IEEE 802.11 MAC protocol, which are shown in table 2.

4.1. Simulation models

In our simulations, we simulated a scenario of 16 mobile hosts active in a square area of 200 m $\times$ 200 m. The initial location of each mobile host is assigned randomly. Each mobile host has three possible transmission ranges of 100 m (2 Mb/s), 60 m (5.5 Mb/s) and 30 m (11 Mb/s) as shown in figure 4. The packet arrival rate of each mobile host follows the Poisson distribution with a mean λ, and the packet length is an exponential distribution with a mean of L slots. The packet mean length is according to the analyzed average network packets on ordinary LAN [18], which is about 50–150 Bytes (i.e., about 10–30 slots in 2 Mb/s transmission rate). These popular TCP/UDP packets occupy overall traffic loading over 74%. Thus, we assume $L = 20$ slots in our simulations. For evaluating the effect of the buffer queuing delay, every mobile host is assumed to equip with infinite buffer space. Each simulation run lasts 200 seconds ($\approx 10^7$ slot times) and each simulation result is obtained by averaging the results from ten independent simulation runs.

In our simulations, we considered two different models. In the first simulation model (model I), hosts are static during whole simulation period. The packet arrival rate of each MH varies from 0.001 to 0.009 in a step of 0.001. In the second simulation model (model II), every host is movable and the packet arrival rate of each MH is 0.001. The moving probability is considered from 0.1 to 1.0 in a step of 0.1. Moving probability 0.1 means one movement will occur in every 10 slots in average. With this simulation model, we investigate three possible moving speeds of a mobile host: 20 m/s (car speed), 10 m/s (race speed) and 6 m/s (jog speed). For simplicity, we assume a mobile host will stay at the new position for a while before its next move. The pause time periods for moving speeds 20 m/s, 10 m/s and 6 m/s are 800 ms, 1600 ms and 2667 ms, respectively. The distance of each movement is 17 m and the move direction is randomly selected from 8 directions.

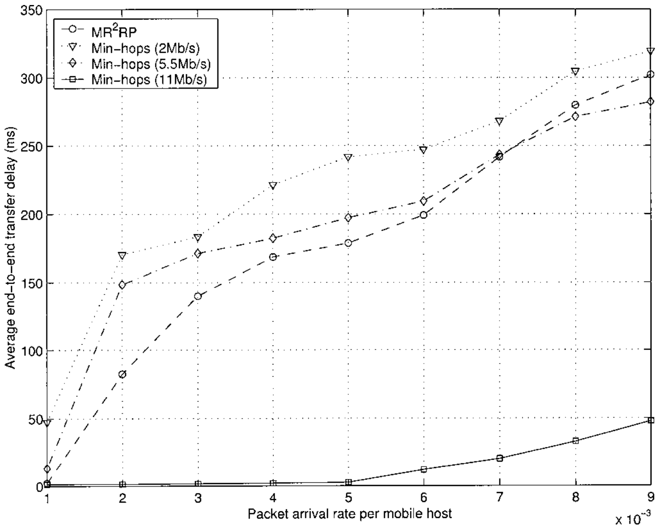

Figure 10. Comparisons of the average transfer delays derived by MR^2RP and Min-hops approach under different packet arrival rates in model I.

In order to evaluate the efficiency of proposed MR^2RP protocol, we investigate four parameters: the average transfer delay (in ms), the average MAC access delay (in ms), the call blocking probability and packet loss ratio. The average transfer delay is defined as the average delay, which including the MAC delay, buffer queuing delay and transmission delay, of a packet travelling from source to destination. In our simulations, we only measure the access delays of success packets during simulation period. The call blocking probability is defined as the ratio of the number of discarded request and the total arrival requests during simulation. A packet will be discarded only when no available path from source to destination can be found in network. The packet loss ratio is the percentage of total arrival packets that packets fail in reaching destination by mobility. For comparisons, the conventional shortest path of Min-hops approach is considered. For a specified transmission rate, the Min-hops approach will route the packets from source to destination by the fixed transmission rate.

4.2. Simulation results

Figure 10 shows the average transfer delays derived by MR^2RP and Min-hops approach in model I under different packet arrival rates. A higher packet arrival rate indicates a higher network load. In figure 10, we can see that the average transfer delay is proportional with packet arrival rate for both MR^2RP and Min-hops approaches. The Min-hops (11 Mb/s) and Min-hops (2 Mb/s) approaches always obtain the smallest and the largest transfer delays respectively. This is because that all packets transmitted in Min-hops (11 Mb/s) and Min-hops (2 Mb/s) are at 11 Mb/s and 2 Mb/s, respectively. One can imagine that the Min-hops (11 Mb/s), which has the shortest transmission distance, will have a less chance to find the highway from source to destination in network. On the other hands, the Min-hops (2 Mb/s) will have the highest possibility to establish the path for every request. Figure 10 also demon-

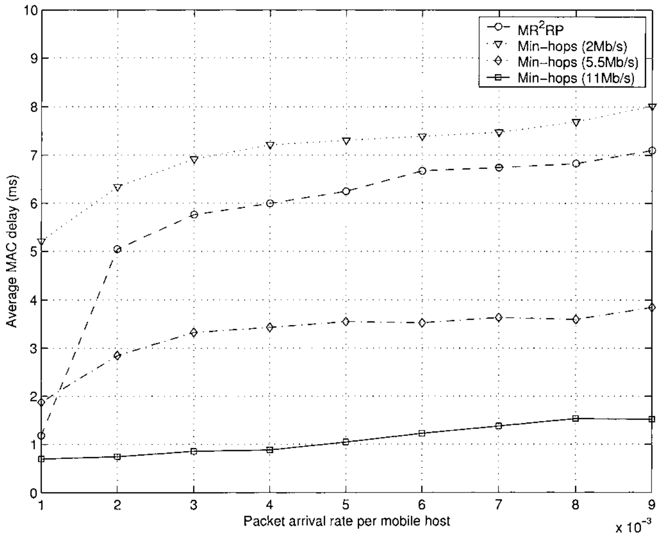

Figure 11. Comparisons of the average MAC delays derived by MR^{2}RP and Min-hops approach under different packet arrival rates in model I.

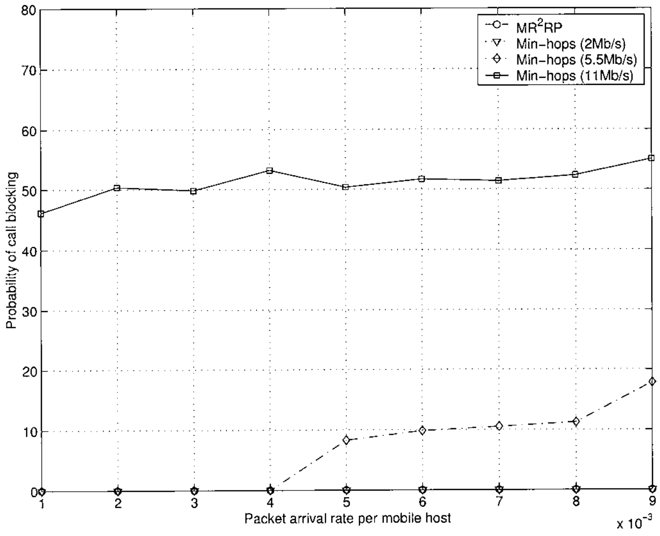

Figure 12. Comparisons of the call blocking probabilities derived by MR^{2}RP and Min-hops approach under different packet arrival rates in model II.

strates the proposed MR^{2}RP always derives a lower average transfer delay than that of Min-hops (2 Mb/s) and the performance of MR^{2}RP is very close to the Min-hops (5.5 Mb/s) in heavy network loaded. This indicates that our MR^{2}RP has the ability to find the path of supporting data rate up to 5.5 Mb/s in average. We also emphasize that the incurred buffer delay along the path may dominate the average transfer delay. This can be seen from the average transfer delay of MR^{2}RP is larger than that of Min-hops (5.5 Mb/s) when the packet arrival rate is larger than 0.007. This result also implies our MR^{2}RP can service more packets than Min-hops (5.5 Mb/s) approach (In fact, the MR^{2}RP is the most efficient protocol on serving packets). The phenomena is resulted from the MR^{2}RP performs load balancing. Recall that MR^{2}RP always selects the best path of the minimal transfer delay for a request at that moment. Once these routes of the minimal transfer delay are occupied, the increasing queue length along the path will make the following routing decision to select the second best route, which may take more hops or select a lower transmission rate but with less buffer delay or less contention. However, the increasing of the number of survived packets will raise the measured transfer delay in our simulation as shown in figure 10. This indicates the load balancing is one of the features of the MR^{2}RP.

Figure 11 illustrates the average MAC delays derived by MR^{2}RP and Min-hops approach in model I under different packet arrival rates. The average MAC delay is also proportional with the network load. We can easily see that the MR^{2}RP will obtain a lower average MAC delay than Min-hops (2 Mb/s) but higher than Min-hops (5.5 Mb/s) and Min-hops (11 Mb/s). We note that the Min-hops (2 Mb/s), whose transmission distance is the longest, has the best chance in finding a path for request. In MR^{2}RP, the worse case for serving a request is to select the path with the lowest transmission rate as Min-hops (2 Mb/s) approach does. Therefore, in the case of no packet lost, the numbers of transmitted packets in MR^{2}RP and in the Min-hops (2 Mb/s) will be the same. Since the MAC delay is relying on the number of competitors, a lower MAC delay means there are less contentions occurring on each transmission attempt. This demonstrates that the proposed delay-oriented MR^{2}RP is able to minimize the contention delay. We also note that when the network load becomes heavy, MR^{2}RP will distribute packets among entire network. Consequently, the queue length of each MH will grow up simultaneously and each transmission will suffer a longer contention resolving. However, due to fewer packets will be serviced by both Min-hops (5.5 Mb/s) and Min-hops (11 Mb/s) (this conclusion will be explained later), the contention on each transmission will be reduced accordingly. This is why the average MAC and transfer delays of MR^{2}RP are obvious higher than that of Min-hops (11 Mb/s) and Min-hops (5.5 Mb/s). We also note that when the packet arrival rate is 0.001 (light load), the MR^{2}RP outperforms than Min-hops (5.5 Mb/s).

Figure 12 illustrates the call blocking probabilities derived by MR^{2}RP and Min-hops approach. As mentioned before, both MR^{2}RP and Min-hops (2 Mb/s) have the same call blocking probability. In this figure, we can see that the call blocking probabilities of them are almost zero. This reason is the considered square area by simulation is only 200 m $\times$ 200 m and the 100 m transmission distance can easily find the path for a pair of MHs in this area. We also can find the call blocking probability of Min-hops (11 Mb/s) is about 50% for all kinds of network load. Also, when the packet arrival rate is larger than 0.005, approach Min-hops (5.5 Mb/s) will block about 10% packet requests. Based on these results shown in figures 10–12, we conclude that the total amount of packets serviced by MR^{2}RP is much more than the Min-hops approach with higher data rates.

Figure 13 shows the derived packet loss ratios of proposed MR^{2}RP and Min-hops (2 Mb/s) approach under different moving probabilities and different moving speeds in model II. In this simulation, packet will be lost when the selected route cannot reach the destination any longer. Obvi-

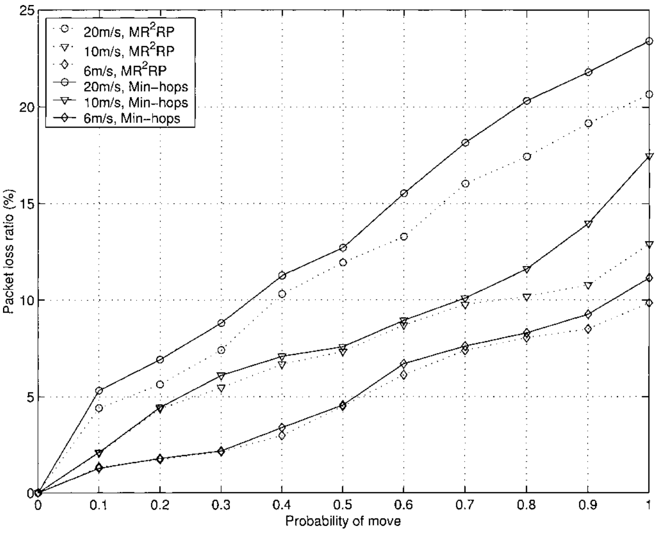

Figure 13. Comparisons of the packet loss ratio derived by MR^{2}RP and Min-hops approach under different moving probabilities in model II.

ously, given a higher moving probability or a faster moving speed, a higher packet loss ratio will be obtained. When the MH moves in a speed of 20 m/s (about 72 km/hr), the packet loss ratio will increase sharply as the increasing of moving probability. From figure 13, we can see that the curves of the MR^{2}RP are still always lower than that of Min-hops (2 Mb/s). This encourages us the proposed MR^{2}RP can provide not only the fastest routing path but also the more reliable routing path for packets in MR^{2}WN.

5. Conclusion

In this paper, we present a new routing protocol, named as the multi-rate and multi-range routing protocol (MR^{2}RP), which can provide an efficient and scalable routing for multi-rate IEEE 802.11 wireless *ad hoc* networks. The precise MAC delay of the IEEE 802.11 CSMA/CA protocol is being estimated. Referring from the MAC delay, transmission delay and buffer queuing delay, the MR^{2}RP will find the fast routing path for packets. Simulation results demonstrated that the total transfer delay from source to destination of each packet and the total amount of serviced packets can be significantly reduced and increased respectively by comparing with the conventional shortest path of minimal hops approach. Furthermore, the packet loss ratio, which is caused by mobility, of MR^{2}RP can be also improved.

This work was supported by the National Science Council, Taiwan, R.O.C., under Contract NSC-89-2218-E-032-012.

References

[1] M.S. Alouini, X. Tang and A.J. Goldsmith, An adaptive modulation scheme for simultaneous voice and data transmission over fading channels, IEEE Journal on Selected Areas in Communications 17(5) (1999) 837–850.

[2] C. Andren and J. Boer, Draft text for the high speed extension of the Standard, doc: IEEE P802.11-98/314 (1998).

[3] C. Andren and M. Webster, CCK Modulation Delivers 11 Mbps for High Rate 802.11 Extension, in: *Proc. Wireless Symposium/Portable by Design Conference* (Spring 1999).

[4] Application Note, Complementary code keying made simple, AN9850, Intersil (October 1999).

[5] M.J. Atallah, *Algorithms and Theory of Computation Handbook* (CRC Press, 1999).

[6] F. Cali, M. Conti and E. Gregori, IEEE 802.11 wireless LAN: capacity analysis and protocol enhancement, in: *Proc. IEEE INFO-COM'98*, San Francisco, GA (April 1998) pp. 142–149.

[7] M.H. Callendar, International mobile telecommunications-2000 standards efforts of the ITU, IEEE Personal Communications 4(4) (August 1997) 6–7.

[8] C. Chien el al., Adaptive radio for multimedia wireless links, IEEE Journal on Selected Areas in Communication 17(5) (1999) 793–813.

[9] Data Sheet, Direct Sequence Spread Spectrum Baseband Processor (HFA3860B), No. 4594, Harris Semiconductor (December 1998).

[10] T.A. ElBatt, S.V. Krishnamurthy, D. Connors and S. Dao, Power management for throughput enhancement in wireless ad hoc networks, in: *Proc. IEEE ICC'2000* (June 2000) pp. 1506–1513.

[11] M.J.E. Golay, Complementary series, IRE Transactions on Information Theory (April 1961) 82–87.

[12] K. Halford, S. Halford, M. Webster and C. Andren, Complementary code keying for RAKE-based indoor wireless communication, in: *Proc. IEEE Internat. Symposium on Circuits and Systems (ISCAS'99)* (1999) pp. 427–430.

[13] J.F. Hayes, Adaptive feedback communications, IEEE Transactions on Communications 16 (1968) pp. 29–34.

[14] IEEE 802.11, Part 11: Wireless LAN Medium Access Control (MAC) and Physical Layer (PHY) specifications, IEEE 802.11 Std. (August 1999).

[15] T. Ikeda, S. Sampei and N. Morinaga, The performance of adaptive modulation with dynamic channel assignment in multimedia traffic, in: *Proc. IEEE ICUPC'98* (1998) pp. 523–527.

[16] D.B. Johnson and D.A. Maltz, Dynamic source routing in ad-hoc wireless networks, in: *Mobile Computing*, eds. T. Imielinski and H. Korth (Kluwer Academic, Dordrecht, 1996) chapter 5, pp. 153–181.

[17] G.E. Keiser, *Local Area Networks* (McGraw-Hill, New York, 1989).

[18] K.M. Khalil, K.Q. Luc and D.V. Wilson, LAN traffic analysis and workload characterization, in: *Proc. 15th Conference on Local Computer Networks* (1990) pp. 112–122.

[19] L. Kleinrock and F. Tobagi, Packet switching in radio channels. Part II – The hidden terminal problem in carrier sense multiple access and the busy tone solution, IEEE Transactions on Communications 23(12) (1975) 1417–1433.

[20] S.-J. Lee and M. Gerla, Dynamic load-aware routing in ad hoc networks, in: *Proc. IEEE ICC'2001,* Vol. 10, Helsinki, Finland (June 2001) pp. 3206–3210.

[21] P. Lettieri and M.B. Srivastava, Adaptive frame length control for improve wireless link range and energy efficiency, in: *Proc. IEEE INFO-COM'98* (1998) pp. 564–571.

[22] S. Murthy and J.J. Garcia-Luna-Aceves, A routing protocol for packet radio networks, in: *Proc. 1st Annual ACM International Conference on Mobile Computing and Networking* (1995) pp. 86–95.

[23] S. Murthy and J.J. Garcia-Luna-Aceves, An efficient routing protocol for wireless networks, Mobile Networks and Applications (MONET) 1(2) (1996) 183–197.

[24] P.Z. Peebles, *Probability, Random Variables and Random Signal Principles*, 2nd ed. (McGraw-Hill, New York, 1987).

[25] C.E. Perkins and P. Bhagwat, Highly dynamic destination-sequence distance-vector routing (DSDV) for mobile computers, in: *Proc. ACM SIGCOMM'94*, London, UK (October 1994).

[26] C.E. Perkins and E.M. Royer, Ad hoc on-demand distance vector routing, in: *Proc. 2nd IEEE Workshop on Mobile Computer Systems and Applications (WMCSA'99)*, New Orleans, LA (February 1999) pp. 90–100.

[27] X. Qiu and K. Chawla, On the performance of adaptive modulation in cellular systems, IEEE Transactions on Communications 47 (June

1999) 884–895.
[28] T.G. Robertazzi, *Computer Networks and Systems, Queuing Theory and Performance Evaluation*, 2nd ed. (Springer, New York, 1994).
[29] E.M. Royer and C.K. Toh, A review of current routing protocols for ad hoc mobile wireless networks, IEEE Personal Communications 6(2) (1999) 46–55.
[30] S.-T Sheu and J. Chen, A novel delay-oriented shortest path routing protocol for mobile ad hoc networks, in: *Proc. IEEE ICC'2001*, Vol. 6, Helsinki, Finland (June 2001) pp. 1930–1934.
[31] S.-T. Sheu, Y.H. Lee, M.H. Chen, Y.C. Yu and Y.C. Huang, PLFC: the packet length fuzzy controller to improve the performance of WLAN under the interference of microwave oven, in: *Proc. IEEE GLOBE-COM'00*, Vol. 3 (November 2000) pp. 1427–1431.
[32] R. Sivaswamy, Multiphase complementary codes, IEEE Transactions on Information Theory 24(5) (1978) 546–552.
[33] C.-C. Tseng and C.-L. Liu, Complementary sets of sequences, IEEE Transactions on Information Theory 18(5) (1972).
[34] B. Vucetic, An adaptive coding scheme for time-varying channels, IEEE Transactions on Communications 39 (May 1991) 653–663.
[35] W.T. Webb and R. Steele, Variable rate QAM for mobile radio, IEEE Transactions on Communications 43 (July 1995) 2223–2230.
[36] M. Webster et al., Harris/Lucent TGb Compromise CCK (11 Mbps) Proposal, doc: IEEE P802.11-98/246 (July 1998).
[37] J. Williams, L. Hanzo and R. Steele, Channel-adaptive modulation, in: *Proc. 6th Internat. Conference Radio Receivers and Associated Systems* (1995) pp. 344–147.

Shiann-Tsong Sheu received the B.S. degree in applied mathematics from National Chung Hsing University, Taiwan, R.O.C., in 1990, and the Ph.D. degree in computer science from National Tsing Hua University, Taiwan, R.O.C., in 1995. Since 1995 he has been an Associate Professor in the Department of Electrical Engineering, Tamkang University, Taiwan, R.O.C. His current research interests include ATM networks, WDM networks, personal communication networks and design and analysis of protocols and algorithms.
E-mail: stsheu@ee.tku.edu.tw

Yihjia Tsai is an Assistant Professor of Department of Computer Science and Information Engineering (CSIE) at the Tamkang University, Taiwan. His teaching and research interests center on high speed network performance analysis and the use of digital network to facilitate teaching and learning. He is one of the creators of the CAPA (Computer Assisted Personalized Approach) system for online assignments now available from the Michigan State University. He has an M.S. and a Ph.D. from Michigan State University in Computer Science.
E-mail: tsai@cs.tku.edu.tw

Jenhui Chen (ACM S'00/IEEE S'99) received the B.S. degree from the Department of Computer Science and Information Engineering (CSIE), Tamkang University, Tamsui, Taipei, Taiwan, R.O.C, in 1998. Currently, he is working toward his Ph.D. degree in the Department of CSIE at Tamkang University. Since 1998, he has been affiliated with the High Speed Network Laboratory (HSNL) of the Department of Electrical Engineering, Tamkang University, and served as both Teaching and Research Assistant in the Department of CSIE. His main research interests include design, analysis and implementation of network protocols, wireless networks, ATM networks, and artificial intelligence.
E-mail: jenhui@cs.tku.edu.tw